Structural and optical properties of pulsed-laser deposited crystalline β-Ga2O3 thin films on silicon

Berencén, Y.; Xie, Y.; Wang, M.; Prucnal, S.; Rebohle, L.; Zhou, S.;

Structural and optical properties of pulsed-laser deposited crystalline β-Ga2O3 thin films on silicon

Structural and optical properties of pulsed-laser deposited crystalline β-Ga$_2$O$_3$ thin films on silicon

Y Berencén,[1,*] Y Xie,[1,2] M Wang,[1,2] S Prucnal,[1] L Rebohle[1] and Shengqiang Zhou[1]

[1]Helmholtz-Zentrum Dresden-Rossendorf, Institute of Ion Beam Physics and Materials Research, Bautzner Landstraße 400, 01328 Dresden, Germany

[2]Technische Universität Dresden, 01062 Dresden, Germany

Crystalline β-Ga$_2$O$_3$ thin films on (100)- and (111)-oriented Si substrates are produced by pulsed laser deposition. The as-deposited thin films are demonstrated to be polycrystalline and contain a slight deficit of oxygen atoms as measured by X-ray diffraction spectroscopy and Rutherford backscattering spectrometry, respectively. The crystallographic orientation of the Si substrate is found to play no role on the ultimate properties of the films. A direct optical band gap of 4.8 eV is determined by temperature-dependent photoluminescence excitation. Temperature-dependent photoluminescence excitation spectra reveal the existence of a deep acceptor level of around 1.1 eV with respect to the valence band related to self-trapped holes. We experimentally demonstrate that point defects in O-poor β-Ga$_2$O$_3$ thin films act as deep donors and the optical transitions are found to take place via recombination of electrons from one of the intrinsic deep donor levels with self-trapped holes located at 1.1 eV above the valence band. The 3.17 eV-ultraviolet photoluminescence is proven to be related to self-trapped holes in a small polaron state between two O(II)-s sites, whereas the two blue (2.98 eV, 2.72 eV) and the green (2.39 eV) luminescence bands are mainly originated from gallium-oxygen vacancy pairs in the (1-) charge state, gallium vacancies in the (2-) charge state and neutral oxygen interstitials, respectively.

Keywords: β-Ga$_2$O$_3$ thin film on silicon, pulsed laser deposition, substrate orientation, photoluminescence

*E-mail: y.berencen@hzdr.de Tel.: +49 351 260 3137, Fax: +49 351 260 3411

1 2 3 4 5 6 7 8 9 10 11 12 13 14 15 16 17 18 19 20 21 22 23 24 25 26 27 28 29 30 31 32 33 34 35 36 37 38 39 40 41 42 43 44 45 46 47 48 49 50 51 52 53 54 55 56 57 58 59 60

1. Introduction

Gallium oxide (Ga_2O_3) lies in the focus of present-day investigations of the so-called ultra-wide band gap semiconductor materials (viz. band gaps wider than 3.4 eV, GaN) [1]. Among the five known crystalline Ga_2O_3 polymorphs labeled as $α$-, $β$-, $γ$-, $δ$-, and $ε$-Ga_2O_3, the thermodynamically stable monoclinic $β$-Ga_2O_3 phase with a melting point of 1795°C [2] is the most investigated because of its wide 4.8-eV band gap and high 8-MV/cm breakdown electric field [3, 4]. These unique properties make $β$-Ga_2O_3 a promising prospect for UV optoelectronic devices and high-power electronic applications [5, 6].

Monoclinic $β$-Ga_2O_3 belongs to the space group 12 (*C2/m*) and its unit cell consists of two inequivalent Ga sites and three inequivalent O sites. Ga(I) and Ga(II) ions are located at distorted tetrahedral and octahedral sites, respectively. O(I) and O(II) are threefold coordinated, while O(III) is fourfold coordinated [7]. This leads to a strong anisotropy of the electrical, magnetic, optical and thermal properties. The lattice parameters are a = 12.2140(3) Å, b = 3.0371(9) Å, c = 5.7981(9) Å, $β$ = 103.83(2) Å[8], and the unit cell possesses two facile cleavage planes parallel to the (100) and (001) planes, which can be used for the mechanical exfoliation-based synthesis of two-dimensional $β$-Ga_2O_3 [9].

The growth of $β$-Ga_2O_3 thin films can be performed using either physical or chemical vapor deposition methods. Several approaches such as electron-beam evaporation [10], atomic layer deposition [11], low-pressure chemical vapor deposition [12], ultrasonic spray pyrolysis [13], sol-gel [14], high-frequency sputtering [15] and pulsed laser deposition (PLD) [16] are typically used. The properties of the resulting films depend on the processing conditions, namely deposition rate, base pressure, growth temperature,

2

annealing conditions, among others. The substrate plays also a crucial role on the ultimate crystalline quality of β-Ga$_2$O$_3$ thin films. Traditionally, c-plane (0001) sapphire is the substrate of choice because of its hardness, chemical stability, broad range of optical transparency and resistance to high temperatures and pressures [17]. However, little attention has been paid to the use of Si substrates despite its ubiquity in the semiconductor industry. Some attempts have so far been reported on the growth of β-Ga$_2$O$_3$ on either (100) or (111) Si substrates using atomic layer deposition [11, 18, 19, 20], metal organic chemical vapor deposition [21] and spin coating methods [22]. In all the reported works, the as-grown Ga$_2$O$_3$ thin films have resulted to be amorphous irrespective of the fabrication methods and the growth conditions. A post-annealing treatment at temperatures in the range of 500-900°C has shown to be required to achieve crystalline Ga$_2$O$_3$ thin films with the desirable β-phase.

Alternatively, the development and optimization of β-Ga$_2$O$_3$ depend on the possibility of correlating fabrication parameters with defect concentration and its energy. It has recently been reported that unintentionally doped (010) β-Ga$_2$O$_3$ reveals a rich spectrum of defect states throughout the band gap which largely define bulk recombination behavior in devices [23]. One of the most powerful techniques for the investigation of point defects in semiconductors is photoluminescence (PL). It can detect point defects with both shallow and deep energy levels, charge states, and many other parameters. As-grown single-crystalline bulk β-Ga$_2$O$_3$ usually exhibits three room-temperature PL bands centered at around 3.40 eV (UV), 2.95 eV (blue), and 2.48 eV (green) which have been reported to be related to electron recombination with a self-trapped hole [24], donor-acceptor-pair transition [25] and donor-acceptor-pair transition involving an unintentionally introduced

3

impurity center such as Si or Sn [26], respectively. More recently, however, theoretical calculations suggest that each of the observed PL bands can unambiguously be explained by electron recombination with a hole trapped in one of the intrinsic point defects [27].

In the present work, the development of crystalline β-Ga$_2$O$_3$ thin films on either (100)- or (111)-oriented Si substrates using pulsed laser deposition is demonstrated. The crystallographic orientation of the Si substrate is found to play no role on the ultimate properties of the films. The correlation between the structural and the optical properties is reported. Based on this correlation and temperature-dependent PL measurements, a model for the defect-related PL bands in O-poor β-Ga$_2$O$_3$ is proposed. This model consists of the recombination of electrons from one of the intrinsic deep donor levels with self-trapped holes located at 1.1 eV above the valence band.

2. Experimental details

β-Ga$_2$O$_3$ thin films were grown on (100)- and (111)-oriented Si substrates by PLD. A 30-mm-diameter and 5-mm-thick highly pure (99.999%) ceramic Ga$_2$O$_3$ target from American Elements company was used. The Ga$_2$O$_3$ target to Si substrate distance was 70 mm. The substrate temperature during deposition was fixed at 800°C. The deposition chamber was pumped down to a base pressure of 2.67 × 10^{-9} mbar. Subsequently, a working pressure of oxygen of 3.91 × 10^{-2} mbar was introduced. A 248-nm KrF excimer laser with a repetition rate of 10 Hz, 4500 pulses and an energy density of 2.4 J/cm^2 was used to deposit about 200-nm thick β-Ga$_2$O$_3$ thin films.

The crystalline structure of the films was investigated by X-ray diffraction analyses (XRD) using a Brucker D8 advance diffractometer with a Cu-target source. The setup uses a Bragg-Brentano-geometry with a graphite secondary monochromator and a scintillator.

Spectroscopic ellipsometry (SE) was used to determine the thickness (d) and refractive index dispersion of the pulsed laser deposited β-Ga$_2$O$_3$ films. The measurements were made using a Woollam M-2000 spectroscopic ellipsometer operating in the energy range of 1-4 eV with a step size of 0.02 eV at a fixed-angle illumination-detection geometry. The ellipsometry data modelling and analysis was performed using commercially available WVASE32 software.

The thickness and composition of the thin films were determined by Rutherford backscattering spectrometry (RBS) using the 1.7 MeV He$^+$ beam of the Rossendorf van de Graff accelerator at a scattering angle of 170°. SIMNRA software [28] was employed to simulate the experimental RBS data.

A 5 μm x 5 μm surface of the samples was inspected by atomic force microscopy (AFM). Tapping mode imaging was implemented in ambient air leading to topographical images of the samples. Gwyddion software was used for visualization and analysis of the experimental data.

The optical properties in the as-deposited β-Ga$_2$O$_3$ thin films were investigated by temperature-dependent PL and photoluminescence excitation (PLE). The measurements were made using a xenon lamp coupled to a monochromator for the selective PL excitation. The emitted PL light from the sample was guided through a set of lenses to a

Jobin Yvon Triax 320 monochromator and then recorded by a Hamamatsu Si photomultiplier. A lock-in amplifier synchronized to an optical chopper at 20 Hz was employed to enhance the signal-to-noise ratio. A closed-cycle helium gas cooling system was used to perform the temperature-dependent measurements in the temperature range of 15–300K.

3. Results and Discussion

3.1. Structural properties

XRD patterns of the as-deposited Ga_2O_3 thin films on (100) and (111) Si substrates are shown in figure 1. Several diffraction peaks indexed to Ga_2O_3 are identified. This reveals the polycrystalline nature of as-deposited Ga_2O_3 thin films on both (100) and (111) Si. Among the identified peaks, the three peaks indexed to (-201), (-402), and (-603) planes indicate the presence of the β phase in the as-deposited Ga_2O_3 samples on both (100)- and (111)-oriented Si substrates. The (-603) peak indexed to Ga_2O_3 deposited on (111) Si was found to be overlapped by the (222) peak belonging to the (111) plane family. As a result of contamination from the sample holder, additional diffraction peaks indexed to WLα and WLβ are observed. In addition, the average crystal size (Dp) for the β-Ga_2O_3//Si(100) and β-Ga_2O_3//Si(111) thin films was determined to be (33 ± 3) nm and (32 ± 3) nm, respectively, as calculated by the Scherrer's formula [29]:

$$Dp = K\lambda/(B cos\,\theta) \quad (1)$$

where K stands for the Scherrer constant, λ is the X-ray wavelength (1.54056 Å), B is the full width at half maximum of an XRD peak and θ is the XRD peak position (one half of 2θ). This suggests that the average crystal size of the as-deposited β-Ga_2O_3 thin films is

6

not affected by the crystallographic orientation of the Si substrate. The average crystal

size of the as-deposited β-Ga$_2$O$_3$ thin films on both (100)- and (111)-oriented Si

substrates was found to be three and a half times larger than that of β-Ga$_2$O$_3$ deposited

on (111) Si by plasma-enhanced atomic layer deposition followed by rapid thermal

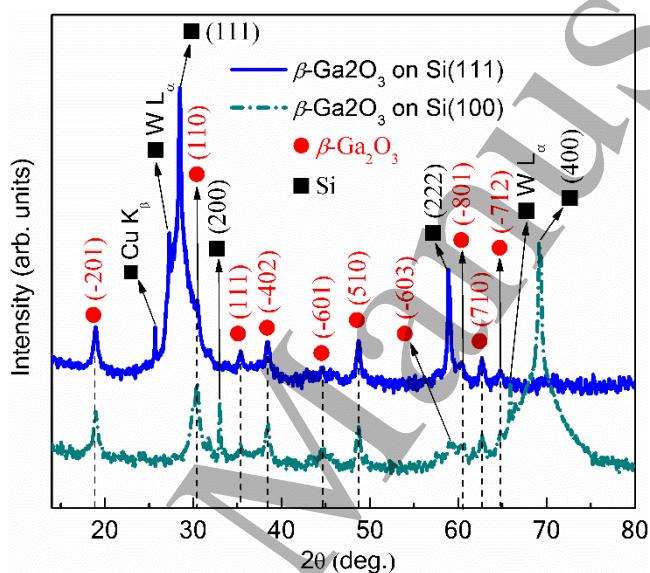annealing at 800°C [19].

Figure 1. XRD patterns of as-deposited β-Ga$_2$O$_3$ thin films on (100)- and (111)-oriented

Si substrates.

The composition and the thickness of samples were quantitatively determined by RBS.

The backscattering spectra of β-Ga$_2$O$_3$ thin films deposited on (100)- and (111)-oriented

Si are illustrated in figure 2(a) and (b), respectively. The measured height and width of

the backscattered Ga signal, which is the heaviest element present in the oxide film, can

be used to determine the concentration of Ga and the thickness of the thin films by using

SIMNRA code. Figures 2(a) and (b) show the good agreement between the simulated

RBS spectra from SIMNRA (solid red lines) and the experimental RBS spectra for both

thin films (open black circles correspond to β-Ga_2O_3//Si(100), while open black squares correspond to β-Ga_2O_3//Si(111)). The resulting thickness for β-Ga_2O_3//Si(100) and β-Ga_2O_3//Si(111) was found to be (208 ± 5) nm and (200 ± 5) nm, respectively. Likewise, the elemetal composition of these β-Ga_2O_3 films was determined to be Ga:41 atom % and O:59 atom %, leading to an O/Ga ratio of 1.43 in both cases (see Table. 1). This is slightly lower compared to the theoretical ratio of 1.50 (Ga:40 atom % and O:60 atom %). These results indicate that these β-Ga_2O_3 thin films suffer from a deficit of oxygen atoms. Theoretical calculations have recently shown that the formation of O vacancies, neutral O interstitials, Ga vacancies, and Ga-O divacancies are the predominant defects in O-poor β-Ga_2O_3 films [27]. This kind of O-poor β-Ga_2O_3 thin films are reported to be one of the materials of choice for gas sensors at high temperature [30].
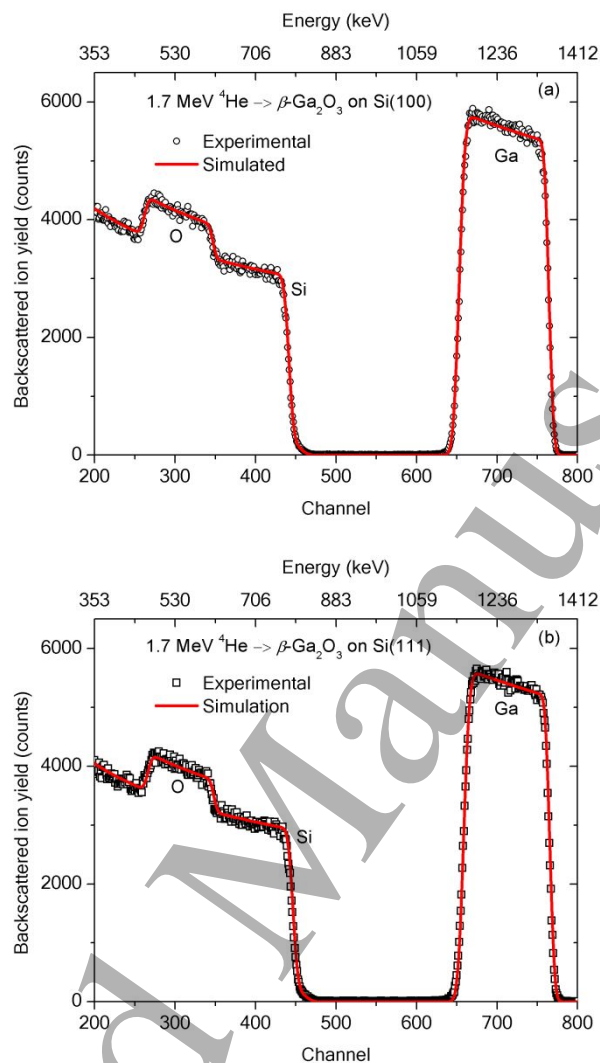
8

Figure 2. RBS spectra of the as-deposited β-Ga$_2$O$_3$ thin films on (100) and (111) Si substrates (a) and (b), respectively. Both the experimental and the simulated curves are shown.

Thickness and refractive index of the thin films were determined by SE. An optical model with a layer stack consisting of a Si substrate and a Ga$_2$O$_3$ film was employed. An extra layer on top of the Ga$_2$O$_3$ film accounting for the surface roughness was considered to properly fit the experimental data. The following empirical Cauchy dispersion model for the refractive index was used [31]:

9

$$n = 1.9044 + 0.01096/\lambda^2 + 0.000587/\lambda^4 \text{ (2)},$$
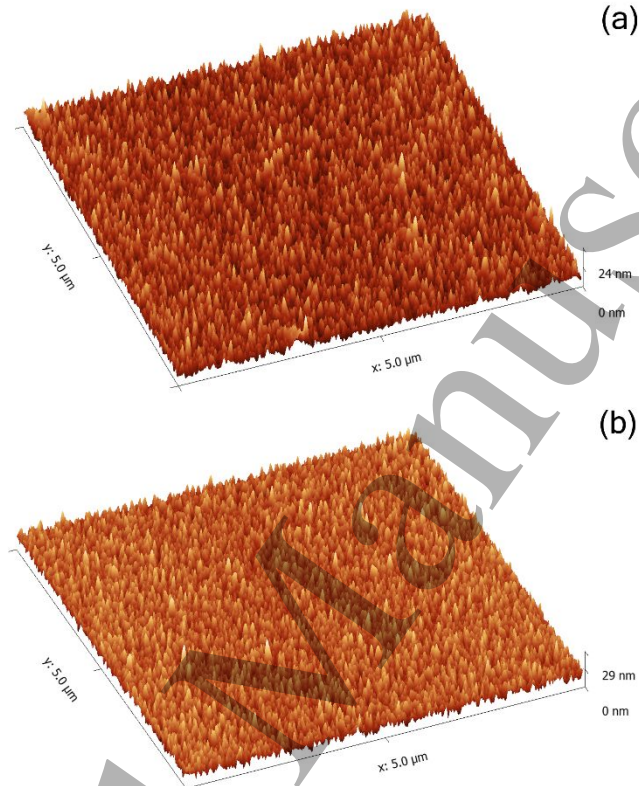
where λ is the wavelength in µm.

Figure 3. Topographical AFM images of the as-deposited β-Ga$_2$O$_3$ thin films on (100) and (111) Si substrates (a) and (b), respectively.

Topographical AFM images reveal no significant differences in terms of surface roughness between the as-deposited β-Ga$_2$O$_3$ thin films on (100)- and (111)-oriented Si substrates (Figure 3). The mean surface roughness for β-Ga$_2$O$_3$ thin films deposited on (100)- and (111)-oriented Si substrates is found to be (2.8 ± 0.3) nm and (3.2 ± 0.3) nm, respectively. This indicates smooth surfaces in both samples.

Table 1 summarizes the deduced film thickness and surface roughness of both as-deposited β-Ga_2O_3 thin films. The film thicknesses determined by SE are in accordance with those estimated by RBS measurements. This confirms the validity of the SE modelling.

Table. 1. Atomic composition, film thickness, surface roughness and average crystal size (D_p) of as-deposited β-Ga_2O_3 thin films on (100)- and (111)-oriented Si substrates as deduced by XRD, RBS, SE and AFM experiments.

sample	O(%)	Ga(%)	O/Ga ratio	d(nm) RBS	d(nm) SE	surface roughness (nm)	Dp (nm)
β-Ga_2O_3//Si (100)	59	41	1.43	208±5	215±3	2.8±0.3	33±3
β-Ga_2O_3//Si (111)	59	41	1.43	200±5	206±3	3.2±0.3	32±3

3.2. Optical properties

To correlate the microstructure with the optical properties, temperature-dependent PLE and PL experiments are performed. β-Ga_2O_3 thin films deposited on either (100)- or (111)-oriented Si substrates show a room-temperature broad PL band centered at around 2.39 eV under 4.80 eV excitation, which spans from 1.85 eV to 3.50 eV (Figure 4(a)). This room-temperature broad emission band is composed of two Gaussian bands centered at 2.42 eV and 2.15 eV, respectively (Figure 4(b)). The 2.42-eV green emission is attributed to neutral oxygen interstitials [32], whereas the red luminescence peaked at 2.15 eV is ascribed to neutral oxygen vacancies [27]. Recently, the formation energy of neutral

11

oxygen vacancies has theoretically been predicted to be lower than that of gallium vacancies, neutral oxygen interstitials and Ga-O divacancies in O-poor β-Ga$_2$O$_3$ [27].

The spectral line shape changes as a function of temperature under 4.8-eV excitation as seen in figure 4(c). A new PL peak centered at around 3.10 eV arises at 200 K and its intensity predominates at 15 K. Two well-resolved peaks in the PLE spectra for the 3.10 eV peak are found to be centered at 4.8 eV and 3.7 eV (Figure 4(c)). The intensity of these two peaks increases as the temperature decreases. The 4.8-eV PLE peak is in well agreement with the reported band gap of β-Ga$_2$O$_3$ [33]. Alternatively, the 3.7-eV PLE band is attributed to self-trapped holes in a small polaron state since this defect-related energy level comes from O(I) sites, which has the lowest formation energy among the other intrinsic defects in O-poor β-Ga$_2$O$_3$ layers [27]. No differences in terms of the PL spectral line shape in the range of the investigated temperatures are observed when using either 4.8 eV or 3.7 eV excitation energies (not shown). This indicates that electrons are promoted to the conduction band from either the valence band (4.8 eV excitation) or from a well-defined acceptor level located at around 1.1 eV with respect to the valence band (3.7 eV excitation). Next, electrons de-excite non-radiatively from the conduction band to one of the deep donor levels. Thus, the defect-related PL takes place by the recombination of electrons located at deep donors with self-trapped holes located at 1.1 eV above the valence band.
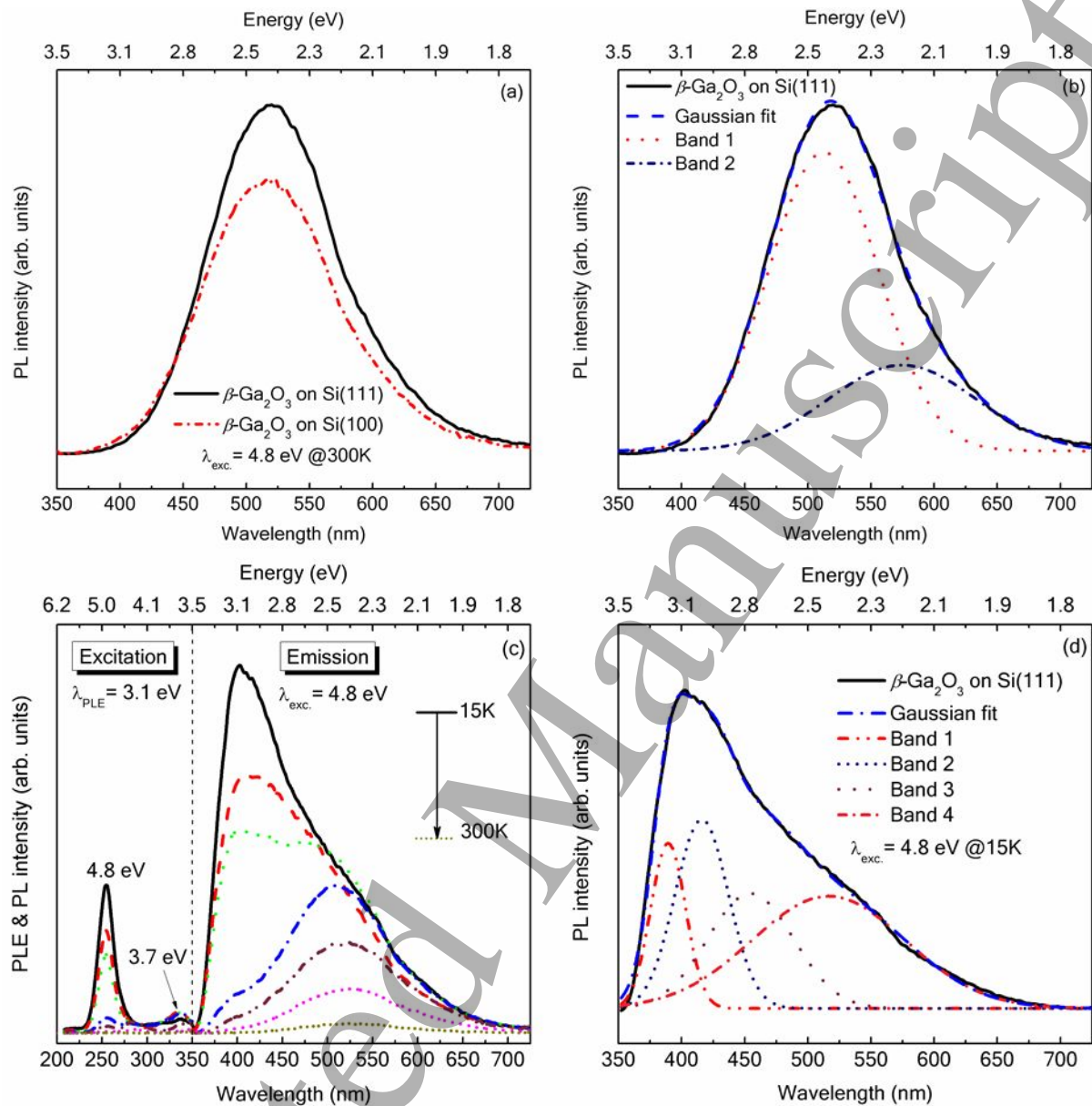
12

Figure 4. (a) Room-temperature PL spectra of as-deposited β-Ga$_2$O$_3$ thin films on (100)- and (111)-oriented Si substrates. (b) Room-temperature deconvoluted PL spectrum of as-deposited β-Ga$_2$O$_3$ thin films on (111)-oriented Si. (c) Temperature-dependent PLE and PL spectra of as-deposited β-Ga$_2$O$_3$ thin films on (111)-oriented Si. (d) Deconvoluted PL spectrum at 15 K of as-deposited β-Ga$_2$O$_3$ thin films on (111)-oriented Si.

13

To further elucidate the origin of the defect-related PL, the PL spectrum at 15 K under 4.8 eV excitation was deconvoluted into four Gaussian bands centered at 3.17 eV, 2.98 eV, 2.72 eV and 2.39 eV (Figure 4(d)). The optical transitions leading to the defect-related PL bands are summarized in figure 5. The UV-blue band at around 3.17 eV comes from the recombination of electrons with self-trapped holes in a small polaron state between two O(II)-s sites [27, 32, 34]. The two blue bands at around 2.98 eV and 2.72 eV are thought to be related to gallium and oxygen vacancy pairs in the (1-) charge state and gallium vacancies in the (2-) charge state, respectively. This is in agreement with theoretical calculations [27] and temperature-dependent cathodoluminescence investigations [31]. Alternatively, the green band peaking at around 2.39 eV is ascribed to neutral oxygen interstitials originated by the splitting with O(I) [27, 32].
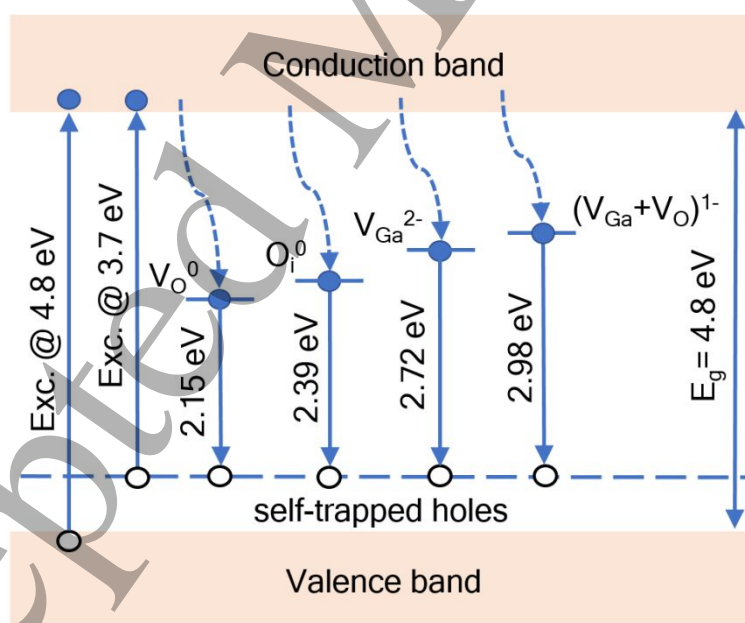

Figure 5. Sketch of the band diagram involving the PL mechanism associated to the different emission bands in crystalline β-Ga$_2$O$_3$ thin films under 3.7 eV and 4.8 eV excitation. Filled circles denote electrons and empty circles denote holes. Curvy arrows

correspond to the non-radiative process of an electron from the conduction band to the specific deep level.

4. Conclusions

In summary, the development of crystalline β-Ga_2O_3 thin films on either (100)- or (111)-oriented Si substrates by PLD has been demonstrated. The resulting films have been determined to be polycrystalline with a deficit of oxygen atoms. No differences in terms of the structural and the optical properties of the films with the crystallographic orientation of the Si substrate have been found. From the industrial standpoint, this might lead to more flexibility for the fabrication of β-Ga_2O_3-based devices using either 100- or 111-oriented Si substrates. A direct optical band gap of 4.8 eV has been determined by temperature-dependent PLE measurements. The sub-band gap PL excitation at 3.7 eV of β-Ga_2O_3 films has been correlated with a deep acceptor level located at around 1.1 eV with respect to the valence band, originating from self-trapped holes. Four defect-related PL bands in the range of 3.17 eV-2.39 eV have been observed at 15 K and ascribed to the recombination of electrons from one of the intrinsic deep levels with self-trapped holes located at 1.1 eV above the valence band.

Acknowledgments

References

[1] Tsao J Y *et al.* 2018 *Adv. Electron. Mater.* **4** 1600501

[2] Zinkevich M and Aldinger F 2004 *J. Am. Ceram. Soc.* **87** 683

[3] Higashiwaki M and Jessen G H 2018 *Appl. Phys. Lett.* **112** 060401

[4] Pearton S J *et al* 2018 *Appl. Phys. Rev.* **5**, 011301

[5] Hu G C, Shan C X, Zhang N, Jiang M M, Wang S P and Shen D Z 2015 *Opt. Express* **23** 13554

[6] Higashiwaki M, Kuramata A, Murakami H and Kumagai Y 2017 *J. Phys. D: Appl. Phys.* **50** 333002

[7] Geller S 1960 *J. Chem. Phys.* **33** 676

[8] Ahman J, Svensson G and Albertsson J 1996 *Acta Crystallogr. Sect. C-Cryst. Struct. Commun.* **52** 1336

[9] Hwang W S *et al* 2014 *Appl. Phys. Lett.* **104** 203111

[10] Rebien M, Henrion W, Hong M, Mannaerts J P and Fleischer M 2002 *Appl. Phys. Lett.* **81** 250

[11] Comstock D J and Elam J W 2012 *Chem. Mater.* **24** 4011

[12] Rafique S, Han L, Neal A T, Mou S, Tadjer M J, French R H and Zhao H, 2016 *Appl. Phys. Lett.* **109** 132103

[13] Ortiz A, Alonso J C, Andrade E and Urbiola C 2001 *J. Electrochem. Soc.* **148** F26

[14]   Kokubun Y, Miura K, Endo F and Nakagomi S 2007 *Appl. Phys. Lett.* **90** 031912

[15]   Fleischer M, Hanrieder W and Meixner H 1990 *Thin Solid Films* **190** 93

[16]   Yu F -P, Ou S -L and Wuu D -S 2015 *Opt. Mater. Express* **5** 1240

[17]   Bruni F J 2014 *Cryst. Res. Technol.* **1** 10

[18]   Shan F K, Liu G X, Lee W J, Lee G H, Kim I S and Shin B C 2005 *J. Appl. Phys.* **98** 023504

[19]   Altuntas H, Donmez I, Ozgit-Akgun C and Biyikli N, 2014 *J. Alloys Compd.* **593** 190

[20]   Nieminen M, Niinisto L and Rauhala E 1996 *J. Mater. Chem.* **6** 27

[21]   Kim H W and Kim N H 2004 *Mater. Sci. Eng. B* **110** 34

[22]   Xiang Y, Zhou C and Wang W 2017 *J. Alloys Compd.* **699** 1192

[23]   Zhang Z, Farzana E, Arehart A R and Ringel S A 2016 *Appl. Phys. Lett.* **108** 052105

[24]   Liu C *et al* 2018 *Semicond. Sci. Technol.* **33** 095022

[25]   Víllora E G, Yamaga M, Inoue T, Yabasi S, Masui Y, Sugawara T and Fukuda T 2002 *Jpn. J. Appl. Phys.* **41** L622

[26]   Hartwig T and Kellendonk F 1978 *J. Solid State Chem.* **24** 255

[27]   Ho Q D, Frauenheim T and Deák P 2018 *Phys. Rev. B* **97** 115163

[28]   SIMNRA is a program for the simulation of RBS spectra. Further details can be found as follows: Mayer, M. SIMNRA User's Guide, Technical Report IPP 9/113; Max- Planck-Institut fur Plasmaphysik: Garching, Germany, 1997

[29]   Patterson A L 1939 *Phys. Rev.* **56** 978

[30]   Bartic M, Baban C I, Suzuki H, Ogita M and Isai M 2007 *J. Am. Ceram. Soc*. **90** 2879

[31]   Jenkins F A and White H E, Fundamentals of Optics, 4th ed. (McGraw-Hill, Inc., 1981)

[32]   Onuma T, Fujioka S, Yamaguchi T, Higashiwaki M, Sasaki K, Masui T and Honda T 2013 *Appl. Phys. Lett.* **103** 041910

[33]   Yamaga M, Ishikawa T, Yoshida M, Hasegawa T, Víllora E G and Shimamura K 2011 *Phys. Status Solidi C* **8** 2621

[34]   Polyakov A Y *et al.* 2018 *APL Mater.* **6** 096102